

Optoacoustic monitoring of cerebral venous blood oxygenation through intact scalp in large animals

I. Y. Petrov,¹ Y. Petrov,¹ D. S. Prough,² I. Civenaite,¹ D. J. Deyo,² and R. O. Esenaliev^{1,2,3,*}

¹Laboratory for Optical Sensing and Monitoring, Center for Biomedical Engineering, The University of Texas Medical Branch, 301 University Blvd., Galveston, TX 77555-1156, USA

²Department of Anesthesiology, The University of Texas Medical Branch, 301 University Blvd., Galveston, TX 77555-0591, USA

³Department of Neuroscience and Cell Biology, The University of Texas Medical Branch, 301 University Blvd., Galveston, TX 77555-0625, USA

*riesenal@utmb.edu

Abstract: Monitoring (currently invasive) of cerebral venous blood oxygenation is a key to avoiding hypoxia-induced brain injury resulting in death or severe disability. Noninvasive, optoacoustic monitoring of cerebral venous blood oxygenation can potentially replace existing invasive methods. To the best of our knowledge, we report for the first time noninvasive monitoring of cerebral venous blood oxygenation through intact scalp that was validated with invasive, “gold standard” measurements. We performed an *in vivo* study in the sheep superior sagittal sinus (SSS), a large midline cerebral vein, using our novel, multi-wavelength optoacoustic system. The study results demonstrated that: 1) the optoacoustic signal from the sheep SSS is detectable through the thick, intact scalp and skull; 2) the SSS signal amplitude correlated well with wavelength and actual SSS blood oxygenation measured invasively using SSS catheterization, blood sampling, and measurement with “gold standard” CO-Oximeter; 3) the optoacoustically predicted oxygenation strongly correlated with that measured with the CO-Oximeter. Our results indicate that monitoring of cerebral venous blood oxygenation may be performed in humans noninvasively and accurately through the intact scalp using optoacoustic systems because the sheep scalp and skull thickness is comparable to that of humans whereas the sheep SSS is much smaller than that of humans.

©2012 Optical Society of America

OCIS codes: (170.1460) Blood gas monitoring; (170.4580) Optical diagnostics for medicine; (120.3890) Medical optics instrumentation; (170.1610) Clinical applications; (170.6510) Spectroscopy, tissue diagnostics.

References and links

1. S. L. Bratton, R. M. Chestnut, J. Ghajar, F. F. McConnell Hammond, O. A. Harris, R. Hartl, G. T. Manley, A. w. Nemecek, D. W. Newell, G. Rosenthal, J. Schouten, L. Shutter, S. D. Timmons, J. S. Ullman, W. Videtta, J. E. Wilberger, and D. W. Wright, “Guidelines for the management of severe traumatic brain injury. I. Blood pressure and oxygenation,” *J. Neurotrauma* **24**(Supplement 1), S7–S13 (2007).
2. S. L. Bratton, R. M. Chestnut, J. Ghajar, F. F. McConnell Hammond, O. A. Harris, R. Hartl, G. T. Manley, A. w. Nemecek, D. W. Newell, G. Rosenthal, J. Schouten, L. Shutter, S. D. Timmons, J. S. Ullman, W. Videtta, J. E. Wilberger, and D. W. Wright, “Guidelines for the management of severe traumatic brain injury. X. Brain oxygen monitoring and thresholds,” *J. Neurotrauma* **24**(Supplement 1), S65–S70 (2007).
3. S. L. Bratton, R. M. Chestnut, J. Ghajar, F. F. McConnell Hammond, O. A. Harris, R. Hartl, G. T. Manley, A. w. Nemecek, D. W. Newell, G. Rosenthal, J. Schouten, L. Shutter, S. D. Timmons, J. S. Ullman, W. Videtta, J. E. Wilberger, and D. W. Wright, “Guidelines for the management of severe traumatic brain injury. IX. Cerebral perfusion thresholds,” *J. Neurotrauma* **24**(Supplement 1), S59–S64 (2007).

4. S. P. Gopinath, C. S. Robertson, C. F. Contant, C. Hayes, Z. Feldman, R. K. Narayan, and R. G. Grossman, "Jugular venous desaturation and outcome after head injury," *J. Neurol. Neurosurg. Psychiatry* **57**(6), 717–723 (1994).
5. D. S. Prough, V. Yancy, and D. J. Deyo, "Brain monitoring: considerations in patients with craniocerebral missile wounds," in *Missile Wounds of the Head and Neck*, B. Aarabi and H. H. Kaufman, eds., (The American Association of Neurosurgical Surgeons, Rolling Meadows, IL, 1999), 221–253.
6. W. J. Levy, S. Levin, and B. Chance, "Near-infrared measurement of cerebral oxygenation. Correlation with electroencephalographic ischemia during ventricular fibrillation," *Anesthesiology* **83**(4), 738–746 (1995).
7. J. H. Choi, M. Wolf, V. Toronov, U. Wolf, C. Polzonetti, D. Hueber, L. P. Safonova, R. Gupta, A. Michalos, W. Mantulin, and E. Gratton, "Noninvasive determination of the optical properties of adult brain: near-infrared spectroscopy approach," *J. Biomed. Opt.* **9**(1), 221–229 (2004).
8. V. Pollard, D. S. Prough, A. E. DeMelo, D. J. Deyo, T. Uchida, and H. F. Stoddart, "Validation in volunteers of a near-infrared spectroscope for monitoring brain oxygenation *in vivo*," *Anesth. Analg.* **82**(2), 269–277 (1996).
9. V. Pollard, D. S. Prough, A. E. DeMelo, D. J. Deyo, T. Uchida, and R. Widman, "The influence of carbon dioxide and body position on near-infrared spectroscopic assessment of cerebral hemoglobin oxygen saturation," *Anesth. Analg.* **82**(2), 278–287 (1996).
10. V. Pollard and D. S. Prough, "Cerebral oxygenation: near-infrared spectroscopy," in *Principles and Practice of Intensive Care Monitoring*, M. J. Tobin, ed., (McGraw-Hill, New York, 1998), 1019–1033.
11. R. O. Esenaliev, K. V. Larin, I. V. Larina, M. Motamedi, and D. S. Prough, "Optoacoustic technique for non-invasive continuous monitoring of blood oxygenation," in *Biomedical Topical Meetings* (Optical Society of America, Washington DC, 2000), 272–274.
12. R. O. Esenaliev, I. V. Larina, K. V. Larin, D. J. Deyo, M. Motamedi, and D. S. Prough, "Optoacoustic technique for noninvasive monitoring of blood oxygenation: a feasibility study," *Appl. Opt.* **41**(22), 4722–4731 (2002).
13. Y. Y. Petrov, D. S. Prough, D. J. Deyo, M. Klasing, M. Motamedi, and R. O. Esenaliev, "Optoacoustic, noninvasive, real-time, continuous monitoring of cerebral blood oxygenation: an *in vivo* study in sheep," *Anesthesiology* **102**(1), 69–75 (2005).
14. Y. Y. Petrov, I. Y. Petrova, I. A. Patrikeev, R. O. Esenaliev, and D. S. Prough, "Multiwavelength optoacoustic system for noninvasive monitoring of cerebral venous oxygenation: a pilot clinical test in the internal jugular vein," *Opt. Lett.* **31**(12), 1827–1829 (2006).
15. H. P. Brecht, D. S. Prough, Y. Y. Petrov, I. Patrikeev, I. Y. Petrova, D. J. Deyo, I. Cicenaitis, and R. O. Esenaliev, "*In vivo* monitoring of blood oxygenation in large veins with a triple-wavelength optoacoustic system," *Opt. Express* **15**(24), 16261–16269 (2007).
16. I. Y. Petrova, Y. Y. Petrov, R. O. Esenaliev, D. J. Deyo, I. Cicenaitis, and D. S. Prough, "Noninvasive monitoring of cerebral blood oxygenation in ovine superior sagittal sinus with novel multi-wavelength optoacoustic system," *Opt. Express* **17**(9), 7285–7294 (2009).
17. I. Y. Petrov, Y. Petrov, D. S. Prough, D. J. Deyo, I. Cicenaitis, and R. O. Esenaliev, "Optoacoustic monitoring of cerebral venous blood oxygenation through extracerebral blood," *Biomed. Opt. Express* **3**(1), 125–136 (2012).
18. W.-F. Cheong, S. A. Prael, and A. J. Welch, "A review of the optical properties of biological tissues," *IEEE J. Quantum Electron.* **26**(12), 2166–2185 (1990).
19. S. Jacques, "Optical absorption of hemoglobin," Oregon Medical Laser Center, <http://omlc.ogi.edu/spectra/hemoglobin/index.html>.
20. Y. Y. Petrov, D. S. Prough, D. J. Deyo, I. Y. Petrova, M. Motamedi, and R. O. Esenaliev, "*In vivo* noninvasive monitoring of cerebral blood oxygenation with optoacoustic technique," in *Proceedings of the 26th Intern. Conf. of IEEE EMBS* (Inst. of Electr. and Electronics Engineers, NY, 2004), 2052–2054.
21. S. Jacques, "Optical absorption of melanin," Oregon Medical Laser Center, <http://omlc.ogi.edu/spectra/melanin/mua.html>.
22. G. M. Hale and M. R. Querry, "Optical constants of water in the 200-nm to 200- μ m wavelength region," *Appl. Opt.* **12**(3), 555–563 (1973).
23. ANSI Z136, 1 – 2000" in *American national standard for safe use of lasers* (The Laser Institute of America, Orlando, FL, 2000).
24. P. Taroni, D. Comelli, A. Farina, A. Pifferi, and A. Kienle, "Time-resolved diffuse optical spectroscopy of small tissue samples," *Opt. Express* **15**(6), 3301–3311 (2007).
25. V. V. Tuchin, *Tissue Optics: Light scattering methods and instruments for medical diagnostics*, 2nd ed. (SPIE Press, Bellingham, WA, 2007).
26. F. J. Fry and J. E. Barger, "Acoustical properties of the human skull," *J. Acoust. Soc. Am.* **63**(5), 1576–1590 (1978).
27. J. Enderle, S. Blanchard, and J. Bronzino, *Introduction to Biomedical Engineering* (Academic Press, San Diego, CA, 2000), Chap. 15.
28. K. Passler, R. Nuster, S. Gratt, P. Burgholzer, and G. Paltauf, "Piezoelectric annular array for large depth of field photoacoustic imaging," *Biomed. Opt. Express* **2**(9), 2655–2664 (2011).
29. V. G. Andreev, Y. Y. Petrov, D. S. Prough, I. Y. Petrova, and R. O. Esenaliev, "Novel optoacoustic array for noninvasive monitoring of blood parameters," *Proc. SPIE* **7177**, 71770O, 71770O-6 (2009).
30. A. Taruttis, E. Herzog, D. Razansky, and V. Ntziachristos, "Real-time imaging of cardiovascular dynamics and circulating gold nanorods with multispectral optoacoustic tomography," *Opt. Express* **18**(19), 19592–19602 (2010).

31. J. Jose, R. G. H. Willeminck, S. Resink, D. Piras, J. C. G. van Hespén, C. H. Slump, W. Steenbergen, T. G. van Leeuwen, and S. Manohar, "Passive element enriched photoacoustic computed tomography (PER PACT) for simultaneous imaging of acoustic propagation properties and light absorption," *Opt. Express* **19**(3), 2093–2104 (2011).
 32. I. Y. Petrova, Y. Y. Petrov, D. S. Prough, and R. O. Esenaliev, "Clinical tests of highly portable, 2-lb, laser diode-based, noninvasive, optoacoustic hemoglobin monitor," *Proc. SPIE* **7177**, 717705, 717705-6 (2009).
 33. E. I. Galanzha, E. V. Shashkov, P. M. Spring, J. Y. Suen, and V. P. Zharov, "In vivo, noninvasive, label-free detection and eradication of circulating metastatic melanoma cells using two-color photoacoustic flow cytometry with a diode laser," *Cancer Res.* **69**(20), 7926–7934 (2009).
-

1. Introduction

An essential step in reducing adverse outcomes (death or severe neurologic disability) in patients with traumatic brain injury as well as in patients undergoing cardiac surgery is prompt initiation of medical interventions that reduce the likelihood of secondary ischemic brain injury. For all these patients, prompt recognition of low cerebral venous blood oxygenation (low hemoglobin oxygen saturation) is a key to avoiding secondary brain injury associated with brain hypoxia [1]. In specialized clinical research centers, invasive monitoring of cerebral blood oxygenation using jugular venous bulb catheters or brain tissue oxygen tension using intracranial oxygen electrodes have been used to provide prognostic information in these patients and to guide management of the cerebral circulation [2]. However, placement of jugular venous bulb catheters or intracranial oxygen electrodes is reserved for severely head-injured patients. Moreover, both methods require considerable technical expertise to acquire and maintain good-quality monitoring data. Cerebral venous blood oxygenation below 50% (normal range is 55 – 75%) measured in the jugular bulb strongly correlates with poor clinical outcome [3–5]. However, this technique is used only in a limited number of specialized centers with highly trained neurointensivists. Moreover, it requires frequent recalibration and there is significant risk associated with infection, thrombosis, and perforation of the carotid artery. Noninvasive, continuous monitoring of cerebral venous blood oxygenation would be invaluable for management of cerebral ischemia in large populations of the patients with traumatic brain injury and patients undergoing cardiac surgery.

Encouraging reports of NIR spectroscopy use [6, 7] must be balanced against the fact that current technology is qualitative and can be used only as a trend monitor. NIR spectroscopy has yet to provide quantitative measurement of cerebral venous oxygenation [8–10], at least in part because the technique assesses oxygenation of all blood (arterial, capillary, and venous) in the tissue and cannot distinguish venous from arterial and capillary blood.

To provide an alternative to invasive monitoring of cerebral venous blood oxygenation and to facilitate this monitoring in a much higher proportion of head-injured patients, both severely injured and moderately injured, we proposed a noninvasive, quantitative, optoacoustic cerebral venous oxygenation monitor [11, 12]. The optoacoustic technique is based on detection of ultrasound waves generated in tissue by the absorption of optical pulses followed by the thermo-elastic expansion of the absorbing volumes. Our *in vitro* and *in vivo* studies demonstrated the potential of this technique in clinical use [13–15]. Recently, we reported high accuracy of cerebral venous oxygenation monitoring in large animals (sheep) by probing the superior sagittal sinus (SSS), a large central cerebral vein that drains all blood from the brain [16, 17]. In those studies, the scalp was removed at the site of the optoacoustic probing and the measurements were performed through the exposed skull. In this paper, for the first time to our best knowledge, optoacoustic monitoring of cerebral venous blood oxygenation was performed in large animals through the intact scalp and confirmed with blood samples obtained from the SSS using catheters and analyzed with the "gold standard" CO-Oximetry. The study was conducted using our novel, multi-wavelength, portable optoacoustic system. The sheep have a thick scalp and skull (4 mm and 6 mm), which are comparable in thickness to that of humans (4 and 8-10 mm, respectively), while the sheep SSS size (1-2 mm) is much smaller than that of humans (10 mm).

2. Materials and methods

We developed a multi-wavelength optoacoustic system based on a compact optical parametric oscillator (OPO) (Opolette 532 II, Oportek Inc., Carlsbad, CA). The OPO provided pulsed tunable NIR radiation in the range of 680-2400 nm with pulse duration of 10 ns and repetition rate of 20 Hz. We designed and built a sensitive, wide-band optoacoustic probe, which combined a piezoelectric transducer for optoacoustic wave detection and a fiber-optic system for light delivery to tissue. The transducer had a resonance frequency of 2 MHz, bandwidth of 3 MHz, sensitivity of 40 $\mu\text{V}/\text{Pa}$, area of 10 mm² and thickness of 1 mm. The light delivery system incorporated 4 fibers with a core diameter of 1 mm around the transducer [16]. The transducer signals were amplified, digitized with a 100-MHz digitizer (National Instruments Corp., Austin, TX), and then processed in real time by a laptop computer using a custom-written software developed in our lab. The laptop was also used to control the OPO using manufacturer-supplied software.

The system was calibrated using heparinized sheep blood with different oxygenations in a phantom simulating blood vessel in a strongly scattering tissue [16]. Optoacoustic measurements were carried out at wavelengths of 700, 805, and 1064 nm. During the calibration procedure, the optoacoustic signals were recorded from blood simultaneously with blood sampling. A ratio of the blood signal amplitudes obtained at 1064 nm to that obtained at 700 nm were plotted against blood oxygenation measured using a CO-Oximeter (IL 682, Instrumentation Laboratories, Lexington, MA), the “gold standard” technique. This dependence represents a calibration curve that was used in this and our earlier studies [16, 17] to predict SSS blood oxygenation.

We used the system for *in vivo* experiments in six merino sheep in which we performed measurements at the same three wavelengths: 700, 805, and 1064 nm. We chose 700 and 1064 nm because hemoglobin absorption is strongly dependent on oxygenation at these wavelengths, while melanin and water absorption in tissues is relatively low [18–22]. At 1064 nm the hemoglobin absorption increases with oxygenation, while at 700 nm it decreases. Since hemoglobin absorption does not depend on oxygenation at 805 nm (which is the isosbestic point at which oxygenated and deoxygenated hemoglobin absorb light equally), we used signals measured at this wavelength as a reference for signal normalization. To minimize electronic noise, we averaged 400 signals at each wavelength. At a 20-Hz pulse repetition rate, one three-wavelength measurement required 1.5-2 min.

Adult merino sheep was chosen as an animal model for these studies because the animals have a thick scalp and skull (4 mm and 6 mm, respectively), which are comparable in thickness to those of humans (4 and 8-10 mm, respectively). The Institutional Animal Care and Use Committee of the University of Texas Medical Branch (UTMB) approved a protocol for this study. The animals were housed in the Animal Resources Center of UTMB under the daily supervision of veterinarians. The sheep were anesthetized with a 1.5% to 2.0% isoflurane during the study and kept in a prone position. Tracheal intubation was performed for the delivery of both isoflurane and gas mixtures of medical grade oxygen and nitrogen. In each sheep, we performed 2-3 cycles of changes in SSS blood oxygenation by varying the fraction of oxygen (FiO_2) in the inhaled gas mixture from 1.0 to 0.1 and back to 1.0. This resulted in variation of SSS blood oxygenation between 20% and 100%.

To insert a catheter into the SSS, a small craniotomy was performed close to the site of optoacoustic measurements. Blood samples were taken from the SSS immediately after each three-wavelength optoacoustic measurement to obtain the actual value of the SSS blood oxygenation using the CO-Oximeter. The optoacoustic measurements were performed through the intact, shaved scalp and, for comparison, without the scalp. The optoacoustic probe was placed in contact with the tissue and moved over the SSS using a 3D translation stage to obtain SSS signals with the greatest amplitude. To provide good acoustic contact, a thin layer of ultrasound gel was applied between the probe and tissue surfaces. The incident

laser fluence at the site of probing was about 4 mJ/cm^2 , which is well below the maximum permissible exposure for skin in this spectral range (20 to 100 mJ/cm^2 [23]).

During the study we continuously monitored the vital signs of the animals. Blood pressure was measured using a catheter inserted into femoral artery, while arterial blood oxygenation was monitored using a pulse oximeter attached to the lip, tongue, or ear. The cardiac rhythm and heartbeat rate were monitored by electrocardiography. At the end of the experiment the animals were euthanized by using saturated KCl solution intravenously (about 1 cc/kg) under deep isoflurane anesthesia.

3. Results

Figure 1 shows typical optoacoustic signals recorded from the exposed sheep skull over the SSS at the wavelengths of 700 nm (a), 805 nm (b), and 1064 nm (c). There are three signals in each graph for three different oxygenation levels: the blue line shows the signal recorded soon after the start of the oxygenation change cycle (oxygenation level was 65%), the green line represents the signal acquired when oxygenation level became very low (22%), and the red line depicts the signal recorded at the end of the cycle (oxygenation level was high again, 80%).

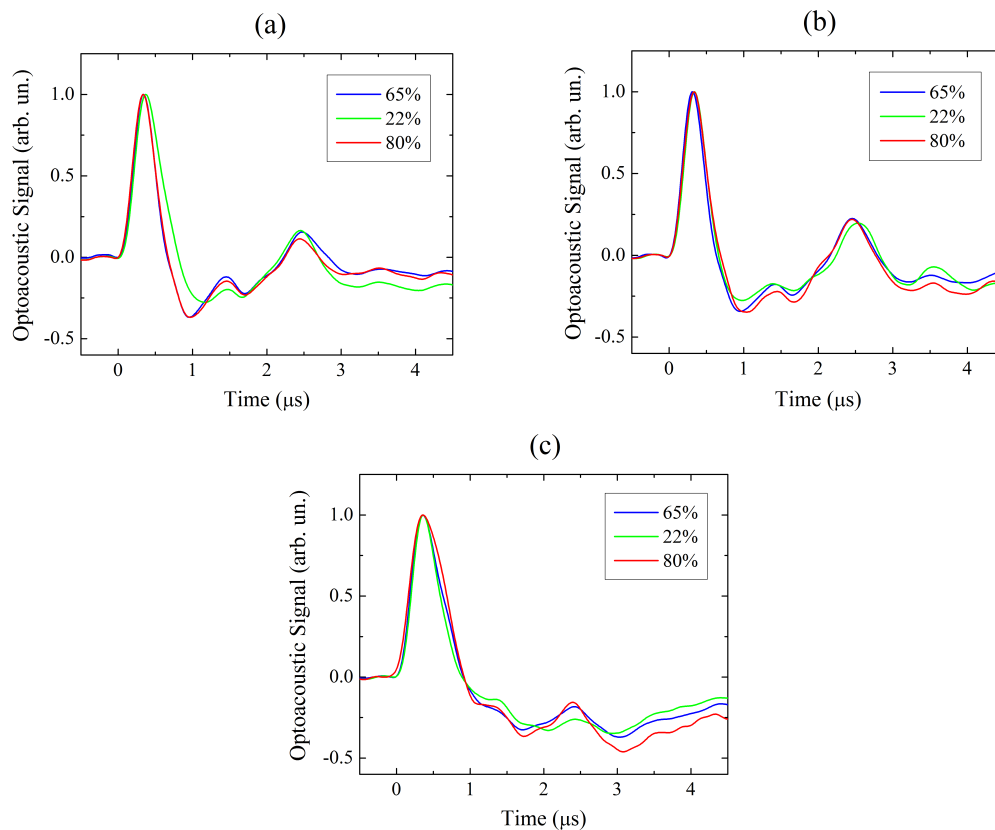


Fig. 1. Optoacoustic signals from the exposed sheep skull and the SSS at wavelengths of 700 nm (a), 805 nm (b), and 1064 nm (c) for different SSS blood oxygenation: 65% (blue line), 22% (green line), and 80% (red line).

The leftmost peak in each signal was produced by the absorption of light in the upper layers of the skull (in the near IR spectral range, the major absorbers within the skull bone are lipids, water, hemoglobin, and collagen [24, 25]). The next prominent peak was delayed from the first one by 2-2.35 μs in different sheep. This time delay can be converted into tissue

thickness by multiplying by the speed of sound in tissue, c_s . Fry et al. [26] reported $c_s = 2.5$ mm/ μ s for the diploe (porous internal layer of the bone) and 2.9 mm/ μ s for both inner and outer tables, while an average speed of sound in skull bone reported by Enderle is 3.36 mm/ μ s [27]. Based on the reported data, one can estimate the minimal and maximal possible bone thickness as $L_{\min} = 2 \mu\text{s} \times 2.7 \text{ mm}/\mu\text{s} = 5.4 \text{ mm}$ and $L_{\max} = 2.35 \mu\text{s} \times 3.36 \text{ mm}/\mu\text{s} = 8 \text{ mm}$, respectively. These numbers fall in the range of the cranial bone thicknesses we measured after the experiments at the location of the craniotomy: from 5 to 8 mm. The SSS is located directly beneath the skull bone, separated only by the *dura matter*, a thin layer of connective tissue. Since hemoglobin is the major chromophore in the near IR spectral range, one can conclude that the second peak is generated in the blood of the SSS.

Blood content of the upper dense layer of the skull bone is extremely low. Since the optoacoustic amplitude depends on the light fluence and absorption coefficient at these wavelengths, the changes in the amplitude of the surface peak were not produced by the variations of blood oxygenation in the bone. Instead, they were produced by the instability of the light fluence and acoustic contact of the probe with the tissue. To minimize influence on oxygenation measurements of OPO pulse energy and acoustic contact instability (and thus to increase the accuracy of these measurements), we normalized all the acquired signals to the amplitude of the surface peak. After that, we use the peak-to-peak amplitude of the SSS signal (the second peak from the left) for the oxygenation measurements. This amplitude decreased with the SSS oxygenation in signals measured at 700 nm, while at 1064 nm it increased with the SSS oxygenation. The SSS signal peak-to-peak amplitude changed only slightly at 805 nm because this wavelength is the isosbestic point of hemoglobin spectrum in the near-infrared spectral range [18–20]. At this wavelength the optical absorption of blood does not depend on oxygenation and the amplitude of the SSS signal was changing due to motion artifacts and variation in total hemoglobin concentration.

Figure 2 shows typical optoacoustic signals detected by the transducer in contact with the intact scalp over the SSS at 700 nm (a), 805 nm (b), and 1064 nm (c). The three signals in each graph represent data for three different oxygenation levels: 26.5%, 45%, and 93.5% (blue, green, and red line, respectively). The leftmost peak was due to the absorption of light in the scalp upper layers. The signals were normalized for the amplitude of the scalp peak to minimize the influence of pulse energy and acoustic contact instability on the measurements. The central peak is separated in time from the first one by 1.3 μ s that corresponds to a distance in soft tissue ($c_s = 1.5$ mm/ μ s) of 2 mm. The scalp thickness on top of the sheep's head is about 3–4 mm. Since the optoacoustic probe exerted some pressure on the scalp to provide good acoustic contact during the measurement, the scalp was compressed by the probe, making 2 mm a reasonable tissue thickness at the measurement site. Thus, this peak was generated at the scalp and skull bone interface, probably in the blood of emissary veins or in the muscle layer that exists in sheep between the scalp and the skull. The peak from the SSS was at about 4 μ s. We verified its position by comparing the time delay from the skull peak (2.2 μ s) with that measured in subsequent experiments with the skull exposed in the same sheep, where the SSS signal was much more prominent due to a higher fluence reaching the vein. Although not very high in amplitude, the SSS signal was still measurable through the thick scalp and skull (2 mm and 7 mm, respectively, as calculated from the signals).

We measured the SSS signal amplitudes during two cycles of oxygenation change and calculated ratio of the amplitudes to that measured at 805 nm. Figure 3 presents the ratios obtained for 700 nm (blue triangles) and 1064 nm (red circles) vs. SSS blood oxygenation measured invasively. The linear fit correlation coefficients (the straight lines) were $R^2 = 0.712$ for 700 nm and $R^2 = 0.869$ for 1064 nm.

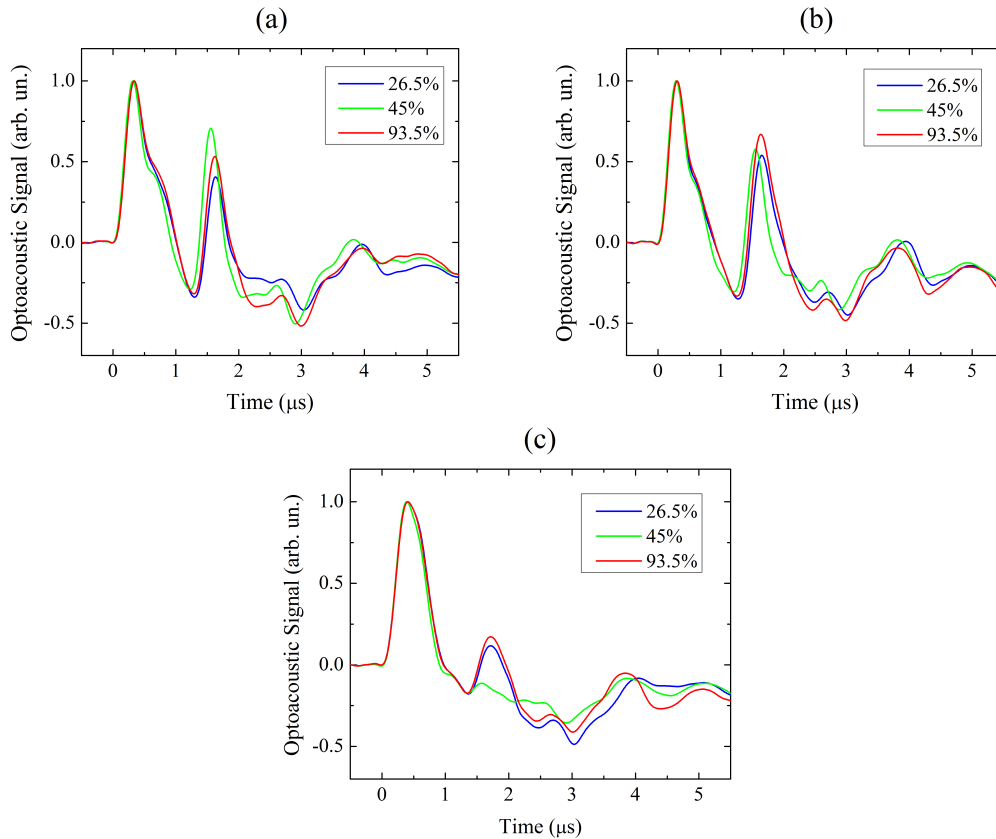


Fig. 2. Optoacoustic signals from a sheep with intact scalp measured at 700 nm (a), 805 nm (b), and 1064 nm (c) for different SSS blood oxygenation: 26.5% (blue line), 45% (green line), and 93.5% (red line).

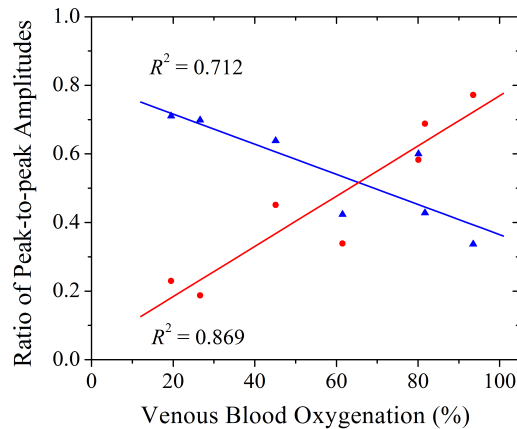


Fig. 3. Correlation of the normalized SSS signal amplitudes measured at 700 nm (blue triangles) and 1064 nm (red circles) with actual SSS blood oxygenation measured invasively. The dashed lines are linear fit to the data sets ($R^2 = 0.712$ and 0.869 for 700 nm and 1064 nm, respectively).

We then used these normalized amplitudes for prediction of blood oxygenation in the SSS using the calibration curve relating the SSS signal amplitude ratio measured at 1064 nm and

700 nm to actual blood oxygenation [16]. We divided the SSS signal amplitude measured at 1064 nm by that measured at 700 nm in Fig. 3 and predicted the SSS blood oxygenation (Fig. 4(a)). The optoacoustically predicted blood oxygenation was linearly dependent on the actual SSS blood oxygenation measured invasively. The linear fit to this set of data points (the straight line) has correlation coefficient $R^2 = 0.931$ and is close to the bisector (the regression coefficient of the line is 0.89).

We analyzed the agreement between the optoacoustically predicted oxygenation and the “gold standard” data obtained with the CO-Oximeter. Figure 4(b) shows the difference between the predicted and actual SSS blood oxygenation in this experiment. The average value of the difference (bias $\langle\Delta\rangle = -5\%$) and the standard deviation from the average (SD = 7.6%) are also shown. The solid line corresponds to the bias value and the two dashed lines delineate the 95% confidence interval $\langle\Delta\rangle \pm 2SD$ (the probability of a data point to fall into this interval is 95%, when all data points are distributed normally). This result is very encouraging when taken into account the presence of the additional thick, turbid tissue layer (the scalp) between the probe and the SSS compared to the data obtained with the exposed skull [16, 17].

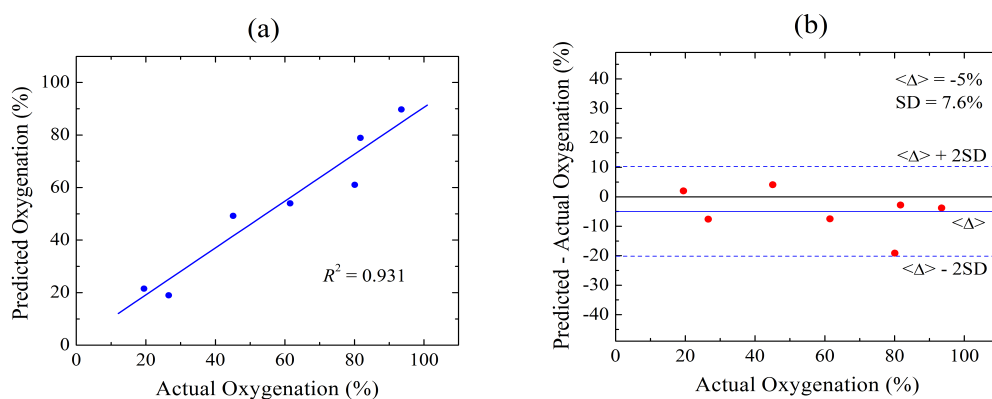


Fig. 4. (a) High correlation between the optoacoustically predicted and actual blood oxygenation in the SSS of a sheep with intact scalp; (b) Standard deviation and bias of the difference between the optoacoustically predicted and actual SSS blood oxygenation.

4. Discussion

In this study we noninvasively measured cerebral venous blood oxygenation in large animals through the intact scalp using our multi-wavelength optoacoustic system. The measurements were validated against blood samples obtained from the catheterized SSS and analyzed with the “gold standard” CO-Oximetry. The SSS signal was easily identified and accurately quantified because the SSS is the largest cerebral vein and there are no other highly absorbing volumes of similar size near the SSS.

Although the attenuation of light by scalp and skull is wavelength-dependent, the calibration of the system in the phantom studies at the same wavelengths minimized its influence on the oxygenation measurements. Although no tissue phantom is ideal for *in vivo* measurements, this calibration provided accurate prediction of the SSS blood oxygenation. This is because the phantom optical properties (the effective attenuation coefficient and its spectral dependence) were very close to those of tissue, and the optoacoustic signals were acquired at different wavelengths within short time. The latter assured that tissue properties did not change significantly during the measurements.

The acoustic waves generated in the SSS blood undergo attenuation and aberration in the skull. However, as we use for predicting the blood oxygenation the ratio of signal amplitudes measured at different wavelengths but in the same geometry, these effects have minimal

influence on the accuracy of the SSS blood oxygenation measurement. The reflections of the SSS acoustic waves from the boundaries of tissue layers (reverberations) arrive at the probe much later than the actual SSS signal and are much stronger attenuated due to a longer path in the tissues and do not reduce accuracy of the SSS oxygenation measurements.

The physiologically relevant range of cerebral venous blood oxygenation for healthy subjects is from 55% to 75%. However, due to traumatic brain injury and instability of blood flow and oxygen consumption in the brain, it varies in a wide range from below 50% to above 75%. We used the range from about 20% to 100% to test the system performance at both normal and abnormal blood oxygenations.

The results that we obtained predict that cerebral venous blood oxygenation may be measured in humans noninvasively and accurately through the intact scalp using optoacoustic systems. By analyzing our *in vivo* data obtained in this and the previous studies [16, 17], we concluded that the major confounding variable in the optoacoustic measurements of the sheep SSS blood oxygenation is due to motion artifacts. Since the probe size ($3 \times 3 \text{ mm}^2$) is comparable to the sheep SSS size (1-2 mm), minor probe displacements by as little as 1 mm can change the SSS signal. Because the adult human SSS is much larger than that of the sheep, we predict that measurements in humans will be substantially less prone to motion artifacts and will be more accurate. Moreover, to avoid the lateral scanning of the optoacoustic probe, one could use optoacoustic arrays for rapid SSS identification and oxygenation measurements. Recently developed optoacoustic arrays providing optoacoustic images deep into highly scattering media and *in vivo* tissues [28–31] could be adapted for SSS signal detection. This would further improve system performance and minimize influence of motion artifacts.

Several other technical modifications could be made to further improve the performance of our optoacoustic system. For instance, using high-power pulsed laser diodes operating at high pulse repetition rate (up to tens of kHz) would substantially reduce measurement time and, thus, increase the measurement accuracy [32,33]. Laser diodes, because of low cost and weight, as well as compact design, are more suitable for the clinical environment than an OPO-based system.

5. Conclusions

We demonstrated that the optoacoustic signal from the large animal SSS is detectable through the thick, intact scalp and skull. The amplitude of the SSS peak correlated well with wavelength and actual SSS blood oxygenation measured invasively: the SSS signal at 700 nm decreased, at 805 nm was almost constant, and at 1064 nm signal increased with oxygenation. To minimize the influence of confounding factors, signal amplitude ratios at 700 nm and 1064 nm to that measured at 805 nm can be used. The optoacoustically predicted values strongly correlated with actual SSS blood oxygenation measured using the CO-Oximeter. Since the sheep scalp and skull thickness is comparable to that of humans and the sheep SSS is much smaller than that of humans, one can predict that cerebral venous blood oxygenation monitoring can be performed in humans noninvasively and accurately through the intact scalp using optoacoustic systems.

Acknowledgments

This work is supported in part by the National Institutes of Health (Grants R01 EB00763 and U54EB007954 from the National Institute of Biomedical Imaging and Bioengineering, Grant R01 NS044345 from the National Institute of Neurological Disorders and Stroke, Grant R41HL10309501 from the National Heart, Lung and Blood Institute), the Moody Center for Brain and Spinal Cord Injury Research/Mission Connect of UTMB, Texas Emerging Technology Fund, and UTMB Seed Grant Program. The content is solely the responsibility of the authors and does not necessarily represent the official views of the NIBIB or NIH. Drs. Prough and Esenaliev are co-owners of Noninvasix, Inc., a UTMB-based startup that has licensed the rights to optoacoustic monitoring technology.